Published online 6 June 2017

Nucleic Acids Research, 2017, Vol. 45, No. 14 ***e133***
doi: 10.1093/nar/gkx514

Determination of tRNA aminoacylation levels by high-throughput sequencing

Molly E. Evans†, Wesley C. Clark†, Guanqun Zheng and Tao Pan*

Department of Biochemistry & Molecular Biology, University of Chicago, Chicago, IL 60637, USA

Received March 31, 2017; Revised May 15, 2017; Editorial Decision May 29, 2017; Accepted May 31, 2017

ABSTRACT

Transfer RNA (tRNA) decodes mRNA codons when aminoacylated (charged) with an amino acid at its 3′ end. Charged tRNAs turn over rapidly in cells, and variations in charged tRNA fractions are known to be a useful parameter in cellular responses to stress. tRNA charging fractions can be measured for individual tRNA species using acid denaturing gels, or comparatively at the genome level using microarrays. These hybridization-based approaches cannot be used for high resolution analysis of mammalian tRNAs due to their large sequence diversity. Here we develop a high-throughput sequencing method that enables accurate determination of charged tRNA fractions at single-base resolution (Charged DM-tRNA-seq). Our method takes advantage of the recently developed DM-tRNA-seq method, but includes additional chemical steps that specifically remove the 3′A residue in uncharged tRNA. Charging fraction is obtained by counting the fraction of A-ending reads versus A+C-ending reads for each tRNA species in the same sequencing reaction. In HEK293T cells, most cytosolic tRNAs are charged at >80% levels, whereas $tRNA^{Ser}$ and $tRNA^{Thr}$ are charged at lower levels. These low charging levels were validated using acid denaturing gels. Our method should be widely applicable for investigations of tRNA charging as a parameter in biological regulation.

INTRODUCTION

Transfer RNAs (tRNAs) are used by the ribosome to translate mRNA into proteins, and the fraction of tRNAs that are aminoacylated (or charged) is an important biological parameter. Both the amount of tRNA and the fraction of charged tRNA affect the speed and efficiency of translation. In *Escherichia coli*, charging levels of different tRNA isoacceptors change upon amino acid starvation (1) which is useful in the translational regulation of stress response proteins in a codon-dependent manner (2). tRNA charging levels also vary during *E. coli* growth where they can act as sensors of cellular metabolism (3,4). Uncharged tRNAs can also trigger the stringent response in bacteria that enables high level synthesis of the alarmone ppGpp (5). In eukaryotes, uncharged tRNA is a well-known activator of the protein kinase GCN2 which phosphorylates eIF2α to regulate global translation activity in response to stress (6). In human cells, tRNA charging levels are affected by proteasome inhibition, which may reflect changes in cellular metabolism when amino acid recycling is ineffective (7).

Two methods have been used in previous attempts to measure tRNA charging levels. Acid-denaturing polyacrylamide gels can, in most cases, separate charged tRNA from uncharged tRNA. After separation, a northern blot is used to determine the charged fraction of a given tRNA species. This method is sensitive but low-throughput: only one tRNA species can be queried at a time (e.g. (8–10)).

tRNA microarrays can also be used to determine charging fraction. Periodate oxidation of the 3′ end is specific to uncharged tRNAs, effectively inactivating the 3′ end for any further enzymatic reaction. After deacylation and subsequent ligation to fluorescent probes, the level of tRNA charging can be ascertained. By comparing untreated sample (total tRNA) to periodate-treated sample (charged tRNA), the charged fraction of tRNA can be determined (1,7,11). While this method can examine the charging of all tRNAs in parallel, the resolution is quite low: an ∼8 nucleotide (nt) difference is required between the DNA probe and tRNA sequence to prevent cross-hybridization. While this specification is not problematic for organisms with low tRNA sequence diversity such as bacteria and yeast, multicellular organisms such as mammals have tRNA isodecoders (same anticodon, different body sequence) with only one or two divergent nucleotides which cannot be resolved on an array (12,13).

Until recently, tRNAs have been resistant to efficient and quantitative high-throughput sequencing because of the large number of modifications and rigid structure. Our lab recently developed DM-tRNA-seq, a method to quantitatively and efficiently sequence tRNA (14). This method

*To whom correspondence should be addressed. Tel: +1 773 702 4179; Fax: +1 773 702 0439; Email: taopan@uchicago.edu
†These authors contributed equally to the paper as first authors.

employs wild-type and mutant *E. coli* AlkB demethylases to remove common Watson–Crick face modifications (m^1G, m^1A, m^3C) in tRNA that commonly cause reverse transcriptase (RT) stops. Additionally, a thermostable reverse transcriptase (TGIRT) is employed to overcome the stable secondary structure. These two features allowed for quantitative high-throughput sequencing of human tRNA from mammalian cells (14). A similar, AlkB-based method was also developed to profile tRNA fragments but does not employ the thermostable TGIRT (15).

Here, we report an extension of the DM-tRNA-seq method to determine the charging fraction of tRNA isodecoders in mammalian cells (Figure 1). Using periodate oxidation followed by treatment at high pH, the 3′ nt of uncharged tRNA is removed through β-elimination while the 3′ nt of charged tRNA is not affected. Thus, tRNAs that were uncharged will end in 3′-CC while tRNAs that were charged will end in 3′-CCA, and a one-pot sequencing reaction can be used to precisely quantify tRNA charging levels of mammalian isodecoders at single-base resolution.

MATERIALS AND METHODS

Cell culture and RNA isolation

Human embryonic kidney HEK293T (CRL-11268) cells from ATCC were grown in Dulbecco's modified Eagle's medium supplemented with 10% Fetal Bovine Serum (FBS), 1% 100 × penicillin-streptomycin and passaged seven times. RNA was extracted once the cells reached 70–90% confluency at P7. RNA was isolated using Trizol, and the pH was maintained at <5 throughout the isolation to prevent hydrolysis of the aminoacyl bond. After ethanol precipitation, total RNA was resuspended in 10 mM NaOac/HOAc pH 4.8, 1 mM ethylenediaminetetraacetic acid (EDTA).

CCA radiolabeling for tRNA standards

tRNA was radiolabeled at the final bridging phosphate with α-^{32}P-ATP and *E. coli* CCA adding enzyme as previously described (16). Briefly, 40 pmol *E. coli* $tRNA^{Tyr}$ (Sigma-Aldrich) was renatured in 20 mM Tris–HCl, pH 7.0 by heating to 85°C for 2 min followed by cooling at room temperature for 3 min. $MgCl_2$ was added to 10 mM, and the tRNA was incubated at 37°C for 5 min. Renatured tRNA was then treated with recombinant, purified *E. coli* CCA adding enzyme (final concentration = 30 μg/ml) at 37°C for 10 min in 50 mM glycine, pH, 9.0, 13 mM $MgCl_2$, 50 μM sodium pyrophosphate, 20 μM cytidine triphosphate (CTP), 0.33 μM α-^{32}P-ATP. Labeled tRNA was purified by denaturing polyacrylamide gelelectrophoresis (PAGE) (7M Urea, 1× Tris-Borate-EDTA (TBE) Buffer).

tRNA standard preparation

Yeast $tRNA^{Phe}$ and *E. coli* $tRNA^{Lys}$ were obtained from Sigma-Aldrich and deacylated before addition to total RNA. *Escherichia coli* $tRNA^{Tyr}$ was *in vitro* charged with total *E. coli* synthetase mix (Sigma-Aldrich). Trace amounts of 3′[^{32}P]A-labeled $tRNA^{Tyr}$ was added to 100 pmol cold $tRNA^{Tyr}$ for charging. The tRNAs were renatured as described above, then treated with total aminoacyl-tRNA synthetase mix from *E. coli* (final concentration = 5.3U/μl) in 40 mM Tris–HCl, pH 7.5, 24 mM KCl, 6 mM dithiothreitol (DTT), 3 mM adenosine triphosphate (ATP), 0.2 mM Tyrosine at 37°C for 15 min. NaOAc/HOAc, pH 4.8 was added to 300 mM, and the reaction was phenol/chloroform extracted before ethanol precipitation. Charged tRNA was resuspended in 50 mM NaOAc/HOAc, pH 4.8, 1 mM EDTA and stored at −80°C for up to 1 month. To determine charging levels of the $tRNA^{Tyr}$ standard, aminoacylated tRNA was digested with P1 nuclease (final concentration = 0.15 U/μl) in 150 mM NH_4OAc pH 4.8 at room temp 20 min. The reaction was resolved on a PEI cellulose TLC plate in 5% acetic acid, 100 mM NH_4Cl. Radiolabeled [^{32}P]pA-Tyr and [^{32}P]pA nucleotides were visualized by autoradiography to determine charging level (Supplementary Figure S1).

Periodate oxidation and β-elimination

Total RNA isolated above was mixed with prepared tRNA standards (final concentration = 0.03 pmol/μg total RNA). Periodate oxidation of total RNA (final concentration = 1 μg/μl) was carried out in 100 mM NaOAc/HOAc, pH 4.8 and freshly prepared 50 mM $NaIO_4$ at room temperature for 30 min. The reaction was quenched with 100 mM glucose for 5 min at room temperature. Any unquenched periodate was removed by Micro Bio-Spin P-6 Columns (Bio-Rad) and two ethanol precipitations. For β-elimination and deacylation, total RNA (final concentration = 1 μg/μl) was treated in 60 mM sodium borate, pH 9.5 at 45°C for 90 min. RNA was purified by Micro Bio-Spin P-6 Columns before ethanol precipitation.

To purify tRNA, total RNA was then run on an 8% denaturing polyacryimide gel (7M Urea, 1× TBE), and tRNA was excised and eluted from the gel in 50 mM KOAc, 200 mM KCl. After ethanol precipitation, short RNA oligo standards were added in different proportions (final concentration = 0.4 pmol total/μg tRNA) to ensure that TGIRT extension from T- and G-ending primers are equivalent. The sequence of the oligo pairs are: first pair:

5′ GUAAUUAUACUCAUAAAUUCGUUGUACGU GAUGCCUAAUUCCUCCA, 5′ GUAAUUAUACUCA UAAAUUCGUUGUACGUGAUGCCUAAUUCCU CC; second pair:

5′ GCGGACUAGGUCCUGUGUUCGAUCCAC AGAGUUCGCACCA, 5′ GCGGACUAGGUCCUG UGUUCGAUCCACAGAGUUCGCACC. In the first biological replicate, the oligos were added in a ratio of 75% 3′-CCA, 25% 3′-CC. In the second biological replicate, oligos were added in equal ratios (50% 3′-CCA, 50% 3′-CC). In the third biological replicate, oligos were added in a ratio of 25% 3′-CCA, 75% 3′-CC. The tRNA and model oligo mixture was used as input for DM-tRNA-seq.

DM-tRNA-seq

This was carried out as previously described (14) with minor modifications. First, tRNA was demethylated under previously optimized conditions. A total of 60 pmol of total tRNA was treated with 120 pmol WT AlkB and 240 pmol

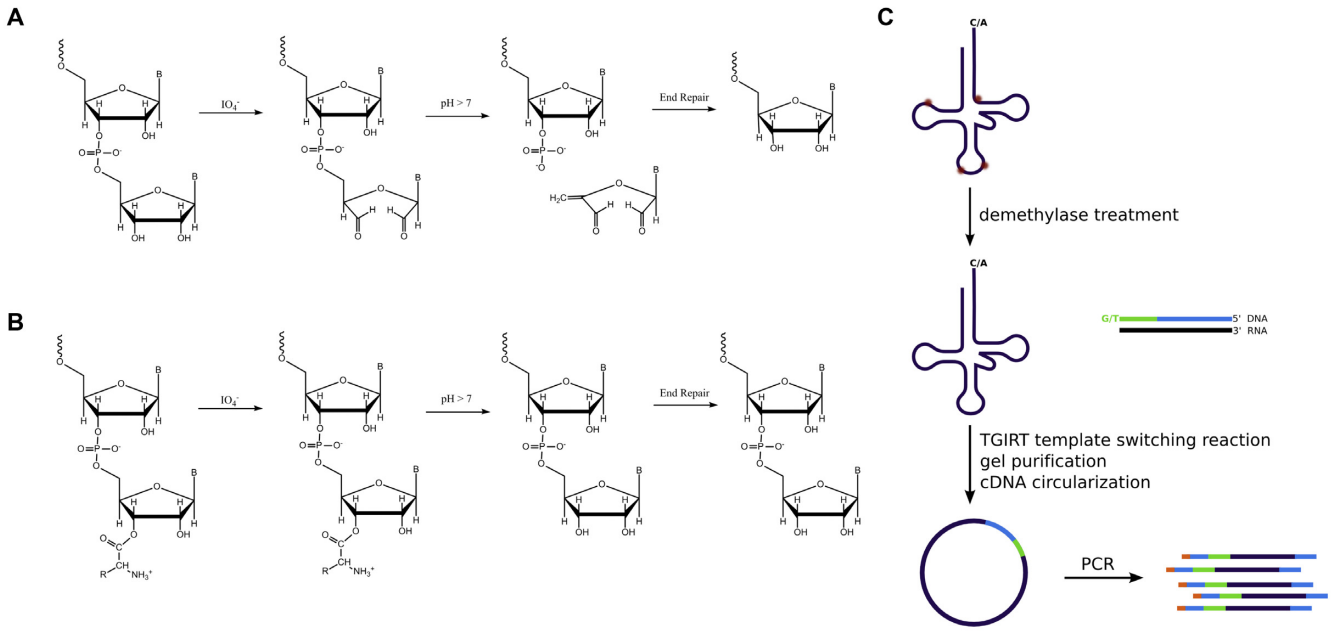

Figure 1. Charged DM-tRNA-seq method. (**A** and **B**) Periodate oxidation and β-elimination can differentiate between charged and uncharged tRNAs before sequencing. Periodate selectively oxidizes the 3′ end of uncharged tRNA (A), while the 3′ end of charged tRNA is protected (B). Treatment with high pH causes β-elimination of the oxidized nucleotide and deacylation of charged tRNA. Thus, after end repair with T4 PNK, charged tRNAs will end in –CCA while uncharged tRNAs will end in –CC. (**C**) Modified DM-tRNA-seq to determine charging fractions. tRNA is first treated with demethylase to remove common tRNA modifications (m^1G, m^1A, m^3C) that impair reverse transcription. Then, a DNA/RNA hybrid with a 1 nt DNA overhang (T/G) is added to act as a primer for the TGIRT template switching reaction. This primer contains binding sites for Illumina PCR/library prep (light blue). For this method, we extended the DNA/RNA hybrid (green) to prevent incorrect assignment of –C and –A ending tRNAs due to *in silico* trimming. After reverse transcription and cDNA purification and circularization, the cDNA is PCR amplified to create a barcoded library for Illumina sequencing.

D135S AlkB in 25 mM MES, pH 5.0, 300 mM KCl, 2 mM $MgCl_2$, 2 mM ascorbic acid, 300 μM α-ketoglutarate, 50 μM $(NH_4)_2Fe(SO_4)_2$ in the presence of RNAsin at room temperature for 2 h. A Zymo RNA Clean and Concentrator kit was used to remove the demethylases and clean up the reaction. Next, end repair (3′ phosphate removal) was performed. A total of 1 μM tRNA was treated with T4 polynucleotide kinase (PNK, Affymetrix) (final concentration = 0.2 U/μl) at 37°C for 30 min. A Zymo RNA Clean and Concentrator kit was again used to clean up the reaction.

For cDNA synthesis, TGIRT primer was 5′ labeled with T4 PNK. A total of 4 pmol of each 5′ labeled TGIRT primer (T-ending: 5′ GATCGTCG GACTGTAGAACTAGACGTGTGCTCTTCCGA TCTTTCAGGCATTAGGCTCAAAGT, G-ending: 5′ GATCGTCGGACTGTAGAACTAGACGTGTGCTC TTCCGATCTTTCAGGCATTAGGCTCAAAGG) was annealed to 8 pmol complementary RNA (5′ CUUUGA GCCUAAUGCCUGAAAGAUCGGAAGAGCACA CGUCUAGUUCUACAGUCCGACGAUC/3SpC3/) in 100 mM Tris–HCl, pH 7.5, 0.5 mM EDTA at 82°C for 2 min, then slow cooled to room temperature. A total of 4 pmol tRNA was then added. The tRNA/primer mixture (200 nM tRNA, 200 nM each primer) was pre-incubated at room temperature for 30 min in 100 mM Tris–HCl, pH 7.5, 450 mM NaCl, 5 mM $MgCl_2$, 5 mM DTT with 500 nM TGIRT (InGex, Inc.). dNTPs were added to a final concentration of 1 mM to initiate the reaction. The reverse transcription was performed at 60°C for 60 min. The reactions were terminated with additions of NaOH to 0.25 M and incubation at 95°C for 3 min. The reaction was neutralized with 0.25 M HCl. An equal volume of 50% Formamide, 4.5M Urea, 50 mM EDTA, 0.05% Bromophenol blue, 0.05% Xylene cyanol was added, and the mixture was heated at 95°C for 15 min.

cDNAs were then purified by denaturing 10% PAGE (7M Urea, 1× TBE), and extended products were cut and eluted from the gel overnight in 50 mM KOAc, 200 mM KCl. Purified cDNA was ethanol precipitated with addition of linear acrylamide (Thermo) to 20 μg/ml.

Purified cDNA was then circularized using CircLigase II (Epicentre) at 60°C overnight. After inactivation at 80°C for 10 min, samples were phenol/chloroform extracted and ethanol precipitated. Polymerase chain reaction (PCR) library preparation for Illumina sequencing was performed using Phusion Master Mix (Thermo) for 12 PCR cycles (98°C 5 s, 60°C 10 s, 72°C 10 s). AMPure XP Beads (Beckman-Coulter) were used to clean up the libraries before Illumina sequencing.

Sequencing analysis

All libraries were sequenced on an Illumina HiSeq 2000 with paired-end mapping using read lengths of 100 base pairs. Standard quality control via FastQC was performed after sequencing and also after read processing. Reads were processed using Trimmomatic v0.32 to remove the standard Illumina adapter sequence followed by subsequent trimming using custom Python scripts to remove demultiplexing

artifacts, primers and trim the extended adapter. This second trimming step ensures that reads are not over-trimmed by Trimmomatic to ensure fidelity of the 3′ end of the raw reads. The resultant trimmed sequences were then aligned to the library using Bowtie 1.0 with sensitive options (–k 1 –v 3 –best –strata). Sequencing reads were aligned to a modified tRNA hg19 genome file, as in (13), containing nuclear-encoded tRNAs, mitochondrial-encoded tRNAs and specific *E. coli* and yeast tRNAs used as standards.

tRNA isodecoder abundance was determined by raw mapped read count for each isodecoder sequence. Because we condensed same-scoring tRNAs from the genomic tRNA database (17) into one sequence, we used only mapped read count for each isodecoder without normalization to the number of genes with the same sequence. Each read was mapped to a single isodecoder based on sequence identity. If a short read could potentially be mapped to multiple isodecoders, it is thrown out due to the mapping ambiguity.

Because Bowtie 1.0 uses end-to-end alignment, the determination for charge ratio is as follows: an aligned read is considered A-ending/charged if it aligns with no mismatches to the tRNA's 3′ 15 nt including the –CCA. Consequently, if the read aligns to the 3′ nt but only ends in –CC, it is considered C-ending/uncharged. Ratios were determined as individual fractional components over the sum of the A-ending and C-ending aligned reads.

Northern blot analysis

Northern probes were 5′ radiolabeled with T4 PNK and gel purified (Trp: 5′ TGACCCCGACGTGATTTGAACACG CAACCTTCTGATCTGGAGTCAGACGCGCTACC GTTGCGCCACGAGGTC, mt-Trp: 5′ CAGAAATTAA GTATTGCAACTTACTGAGGGCTTTGAAGGCTC TTGGTCTGTATTTAACCTAAATTTCT, SerGCT: 5′ GACGAGGRTGGGATTCGAACCCACGYGTGCAG AGCACAATGGATTAGCAGTCCATCGCCTTAAC CACTCGGCCACCTCGT, ThrTGT: 5′ AGGCCCCAGC GAGATTYGAACTCGCGACCCCTGGTTTACAAG ACCAGTGCTCTAACCMCTGAGCTATGGAGCC). A total of 2.5 μg of RNA in 10 mM NaOAc/HOAc, pH 4.8 was mixed with an equal volume 8 M Urea, 0.1 M NaOAc/HOAc, pH 4.8, 0.05% Bromophenol blue, 0.05% Xylene cyanol. A total of 2.5 μg of deacylated RNA (treated in Tris–HCl, pH 9.0 at 37°C for 45 min) was included as a control. Samples were run on a 6.5% PAGE sequencing gel (8M Urea, 0.1M NaOAc/HOAc pH = 5.0) at 500V for 24 h at 4°C. RNA was transferred and fixed to Hybond-XL membrane (GE-Healthcare) using a gel dryer at 80°C for 2 h. The membrane was pre-hybridized twice at room temperature for 30 min in 20 mM sodium phosphate, pH 7.0, 300 mM NaCl, 1% sodium dodecyl sulphate (SDS). Hybridization of radiolabeled oligo (7 pmol) was performed in 20 mM sodium phosphate, pH 7.0, 300 mM NaCl, 1% SDS at 60°C for 16 h. Membranes were washed twice in 20 mM sodium phosphate, pH 7.0, 300 mM NaCl, 0.1%SDS, 2 mM EDTA at 60°C for 20 min. The dried membranes were exposed to imaging plates and quantified using a phosphoimager.

RESULTS AND DISCUSSION

Determining charging fraction by tRNA microarrays relies on selective periodate oxidation of the 3′ end of uncharged tRNAs, essentially inactivating uncharged tRNAs for downstream tRNA labeling with fluorophores (1). However, this approach requires a two-pot reaction: a mock-treated sample measures the level of total tRNA while a periodate-treated sample measures the level of charged tRNAs. We also attempted this approach using DM-tRNA-seq, but the results displayed wide variances due to precise counting of sequencing reads from two separate sequencing libraries (not shown). We therefore devised a new approach by sequencing both charged and uncharged tRNAs in the same library. Instead of only inactivating the 3′ end, we use periodate oxidation coupled to β-elimination of the 3′ oxidized nucleotide to distinguish between charged and uncharged tRNA prior to reverse transcription (Figure 1). In this way, sequencing reads that end in 3′CCA are derived from charged tRNAs while reads that end in 3′CC are derived from uncharged tRNAs.

The procedure starts with total RNA isolated from cells under mildly acidic conditions to prevent hydrolysis of the aminoacyl bond. All mature tRNA ends with 3′CCA. Periodate will only oxidize uncharged tRNAs as the charged tRNAs are protected from oxidation by the covalently attached amino acid. After removal of periodate, β-elimination at slightly basic pH is employed to selectively remove the oxidized 3′A residue, leaving a 3′ phosphate at the terminal 3′C residue (Figure 1A). This 3′ phosphate is then removed using T4 polynucleotide kinase, resulting in 3′C-OH for these uncharged tRNAs. The β-elimination step also deacylates all charged tRNAs, resulting in 3′A-OH for these charged tRNAs (Figure 1B). Demethylase treatment is then carried out to remove Watson–Crick methylations, followed by cDNA synthesis using TGIRT. cDNA is excised from denaturing gels by size, and the library is constructed after circularization and PCR amplification (Figure 1C).

We performed several controls to ensure the completeness of each treatment step (Figure 2). Using a 5′-radiolabeled model oligo, we show that the periodate oxidation followed by β-elimination completely removes the 3′ nt (Figure 2A). Mock treatment with NaCl does not affect the length of the RNA oligo while treatment with $NaIO_4$ shortens the length of the model oligo by 1 nt. This reaction is complete even in the presence of 1 μg/μL total RNA, the condition in which the first steps of the charged tRNA-seq are performed. To ensure complete removal of the 3′ phosphate, yeast tRNA was radiolabeled at the final bridging phosphate using α-^{32}P-ATP and *E. coli* CCA adding enzyme. After periodate treatment, β-elimination and polynucleotide kinase/phosphatase treatment, the 3′ phosphate is completely removed, resulting in the loss of the ^{32}P-signal (Figure 2B). This indicates that the resulting 3′ end of the tRNA is a 3′ hydroxyl group that is required for template switching reaction by TGIRT.

In order to more precisely map the 3′ end of tRNA in the DM-tRNA-seq reaction, we extended the tRNA-seq primer previously used by 20 residues toward the 3′ end of the DNA strand from the Illumina amplification primer binding sites. The TGIRT reaction requires an RNA oligo and its comple-

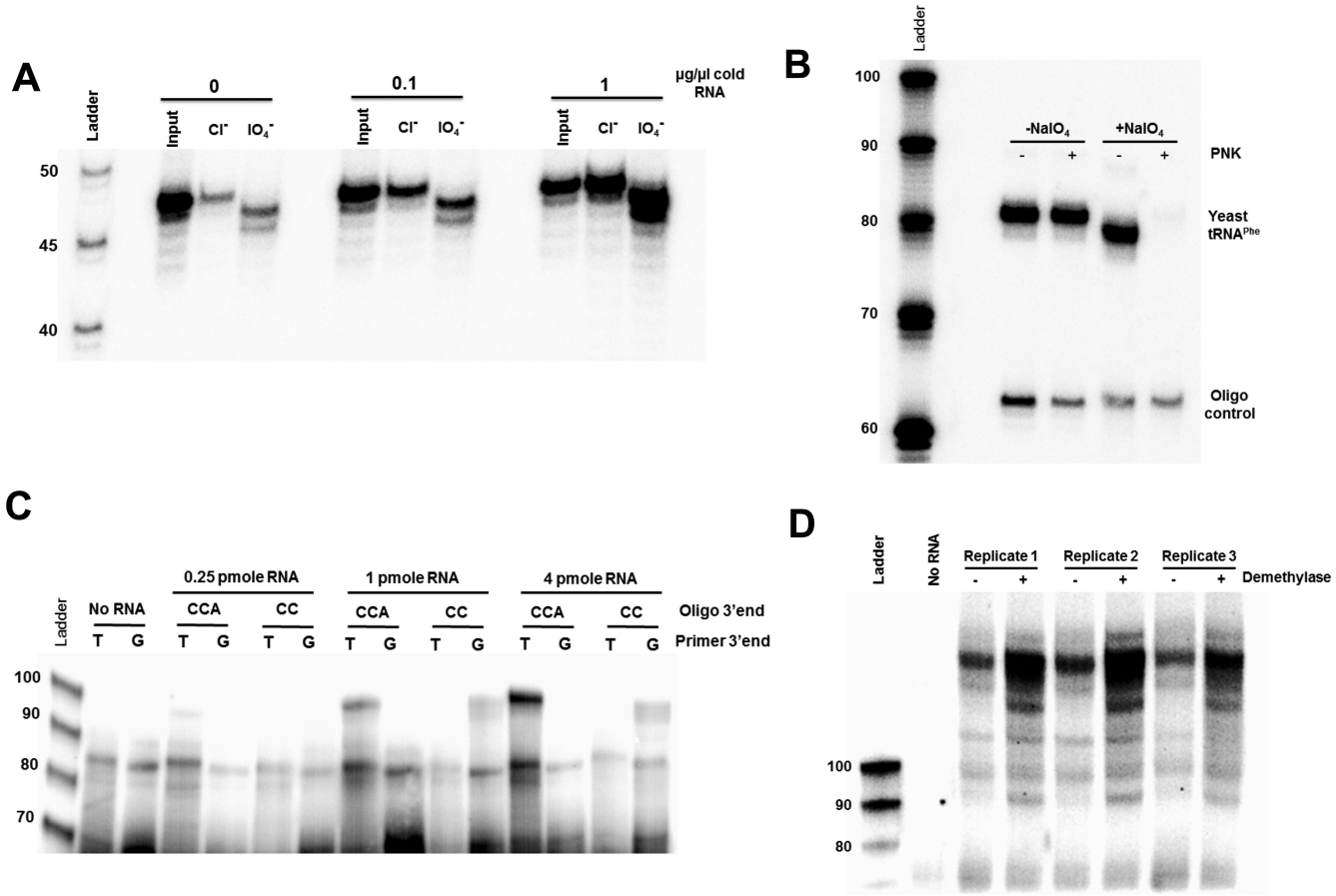

Figure 2. Charged tRNA-seq optimization. (**A**) β-elimination of the final nucleotide is 100%. Using a 5′-radiolabeled model oligo, β-elimination was shown to be complete. After mock treatment with NaCl, the length of the RNA oligo remains the same. However, after treatment with $NaIO_4$, the RNA is 1 nt shorter, even in the presence of 1 μg/μl total RNA. (**B**) Phosphate removal from the 3′ nt is 100%. By labeling the final bridging phosphate, the status of the 3′ end can be monitored. After mock treatment with NaCl, the bridging phosphate remains intact, even with PNK treatment. To remove this phosphate, both $NaIO_4$ and PNK treatment is required. A radiolabeled DNA oligo is included as a reference. (**C**) There is no cross-hybridization of T- and G-ending primers with 3′A- and 3′C-ending oligos. Model oligos were used in order to assess extension of 3′A- and 3′C-ending oligos from T- and G-ending primers. TGIRT will reverse transcribe only when the primers are complementary to the last nucleotide of the oligo (3′C-ending oligo, G-ending primer and 3′A-ending oligo, T-ending primer). The expected cDNA size is 101 nt for the 3′A-ending oligo and 100 nt for the 3′C-ending oligo. The minor product visible in all lanes including no RNA template added (∼85 nt) is likely derived from aberrant RT extension of the RNA and DNA primers in the reaction mixture. (**D**) cDNA from TGIRT reactions that were purified for Illumina sequencing. Treatment with demethylases removes m^1A58, m^1G37 and m^3C32 which are major roadblocks for TGIRT reaction. This allows for sequencing of longer cDNA transcripts, including both full-length tRNA reads and other longer abortive cDNAs caused by TGIRT stops at other modifications and/or the low processivity of TGIRT.

mentary DNA primer (18). Previously, the DNA primer included only Illumina primer binding sites for amplification and a single nucleotide overhang for the template-switching TGIRT reaction (14). In order to prevent *in silico* trimming that may obscure the identity of the 3′ nt, we added a 20 nt 'spacer'. This was designed to ensure compatibility with Illumina barcoding and amplification and prevents misannotation of charged and uncharged tRNAs (Figure 1C). Additionally, to ensure that there is no cross-hybridization between the single nucleotide overhang in the DNA primer and the 3′-end of the RNA, model oligos were used to show that the G-ending DNA primer only extends 3′C-ending RNA while the T-ending DNA primer only extends 3′A-ending RNA (Figure 2C). However, this does not ensure that extension from T- and G-ending primers are equivalent, which is required in order to accurately quantify the charging level. To measure this parameter, two different pairs of model oligos ending in 3′CC and 3′CCA were added in different ratios just before the demethylation step in Figure 1C to compare the measured 3′CCA/3′CC ratio to the input ratio.

To further verify that the measured values of tRNA charging fraction correspond to the actual charging fraction, uncharged *E. coli* $tRNA^{Lys}$ and yeast $tRNA^{Phe}$, and *in vitro* charged *E. coli* $tRNA^{Tyr}$ (62% charged, Supplementary Figure S1) were added to total RNA prior to periodate oxidation. This ensures that periodate oxidation and β-elimination were complete and that charged tRNAs were not deacylated, lending confidence to the measurement of charged tRNA fraction.

We performed charged tRNA-seq using total RNA from HEK293T cells in three biological replicates. After periodate oxidation and β-elimination, DM-tRNA-seq is performed as previously described. The same tRNA samples

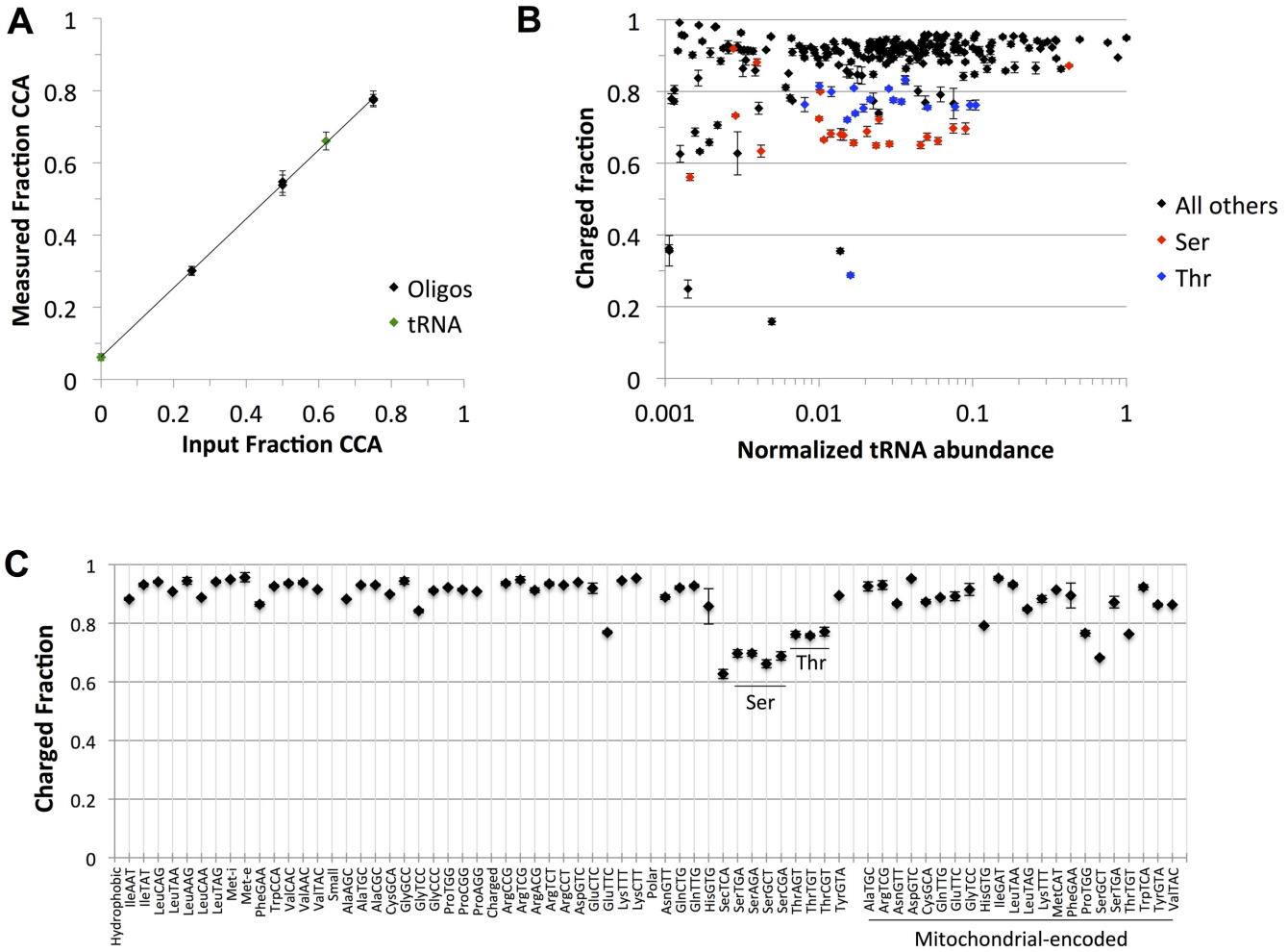

Figure 3. Charged tRNA-seq results. (**A**) Spike-in model oligos and tRNA standards show that charged-tRNA-seq is quantitative. Two pairs of model oligos (black) were added in different molar ratios to the three biological replicates (see 'Materials and Methods' section). Additionally two uncharged tRNAs and one *in vitro* charged tRNA were also added. The 'charged fraction' measured by sequencing was plotted against the input 'charged fraction'. This calibration curve shows that the measured charged fraction is linear across different charged fractions. (**B**) The measured charged fraction is independent of the abundance of tRNA. The abundance of nuclear and mitochondrial-encoded tRNA isodecoders was normalized to the most abundant isodecoder. tRNA isodecoders that were within 1000-fold of the most abundant tRNA were plotted. The charged fraction is independent of the abundance, suggesting that the measured charged fraction should be accurate even for low abundance tRNA isodecoders. $tRNA^{Ser}$ and $tRNA^{Thr}$ isodecoders are highlighted. (**C**) Most abundant tRNA isodecoders are highly charged. The charged fraction of the top abundance isodecoder for each isoacceptor was plotted. Most abundant isodecoders are highly charged (>80%) while $tRNA^{Ser}$ and $tRNA^{Thr}$ isodecoders have lower charging fraction (60–80%).

without demethylase treatment were also sequenced for comparison. cDNA was purified from denaturing gels (Figure 2D), and library construction and tRNA sequence mapping were performed as previously described (14). Approximately 30% of reads from samples that were not treated with demethylase were mapped to genomic tRNA genes, while 45–60% of reads from demethylase treated samples were mapped to genomic tRNA genes (Supplementary Table S1). These mapping statistics are comparable to the original DM-tRNA-seq results (14). The identity for most human tRNA isodecoders can be determined using the sequence of the 30 3′ most nucleotides, so full-length tRNA reads are generally not required to determine tRNA charging fraction for individual isodecoder. However, m^1A58 causes RT stops even for TGIRT and is present in most human tRNAs (19). cDNAs that abort at m^1A58 cover only ∼20 residues of tRNA and can be too short to unambiguously assign to tRNA isodecoders. Thus, in order to properly quantify isodecoder amounts for mammalian samples, demethylase treatment is required. Because of the higher number of mapped reads, demethylase treated samples were used for the remaining analysis. The charged fraction of tRNA isodecoders from demethylase treated replicates correlated well (Supplementary Figure S2), so averages of the three replicates were used for all further analysis.

We first determined the quantitative nature of our experiment using the spike-in standards (Figure 3A). Standards are *E. coli* and yeast tRNAs with known charging fractions and RNA oligo pairs with known 3′A/3′C ratios. All data points have a linear correlation between the expected and measured values ($R^2 = 0.999$) with a slope of 0.955 and in-

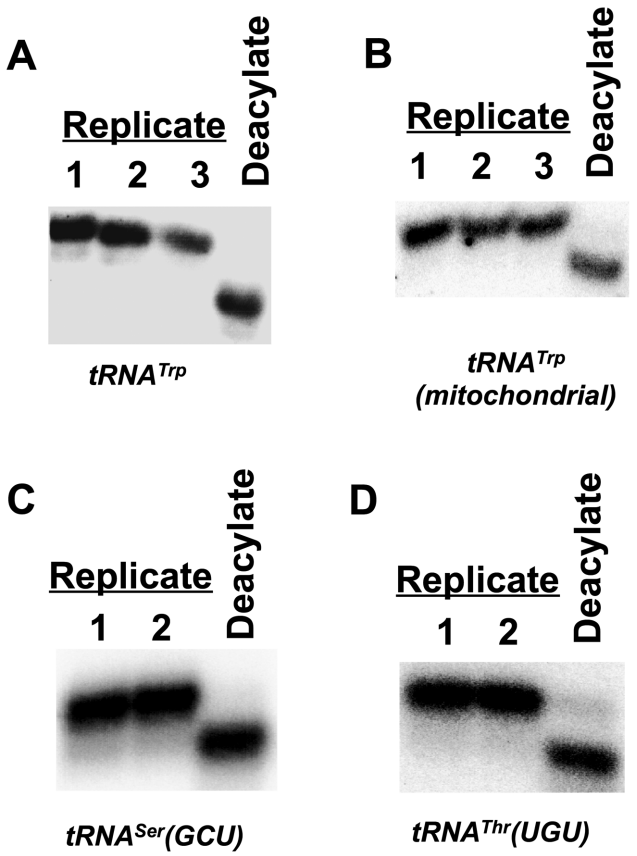

Figure 4. Validation of low charging fraction for $tRNA^{Ser/Thr}$. Total RNA was loaded onto a 6.5% acid denaturing gel to separate charged from uncharged tRNAs. Deacylated RNA was also run as a control. Trp (**A**) and mt-Trp (**B**) are highly charged while $tRNA^{Ser}$(GCU) (**C**) and $tRNA^{Thr}$(UCU) (**D**) have a lower charged fraction. In (C and D), five biological replicates were performed and only two are shown for simplicity.

tercept of 0.06. This result indicates the fully quantitative nature of our method.

We then plotted the charging level of all individual isodecoders that are within a 1000-fold range of the most abundant isodecoder (an initiator $tRNA^{Met}$ in this case, Figure 3B). Most tRNA isodecoders are charged at a level of >80%, consistent with the expected range of charged tRNA fractions in the cell. The small amount of uncharged tRNAs likely resides in the E-site of the ribosome. There is little correlation between tRNA isodecoder abundance and charging fraction within this abundance range, suggesting that our method should be useful to measure charging fraction of all tRNAs, even including rare tRNA isodecoders. On the other hand, the most abundant tRNA isodecoders are typically charged at high levels, indicating that the highly abundant isodecoders are likely used for protein synthesis (Figure 3C). Unexpectedly, $tRNA^{Ser}$ and $tRNA^{Thr}$ isodecoders are charged at lower levels compared to other tRNAs (Figure 3B and C). This result is reminiscent of an *E. coli* study using microarrays where $tRNA^{Ser}$ and $tRNA^{Thr}$ isoacceptors have lower charging levels when grown in media where serine is also heavily used for metabolic purposes (4).

We performed the standard acidic denaturing gel electrophoresis followed by Northern blot to validate the charging levels of several tRNAs, including the unexpected $tRNA^{Ser}$ and $tRNA^{Thr}$ results (Figure 4). High levels of tRNA charging were seen in $tRNA^{Trp}$ (94.0 ± 2.4%, 3 biological replicates) and mt-$tRNA^{Trp}$ (91.0 ± 2.8%, 3 replicates) by Northern blot (Figure 4A and B), agreeing well with values obtained by sequencing for the most abundant $tRNA^{Trp}$ (92.6 ± 0.8%, 3 replicates) and mt-$tRNA^{Trp}$ (92.3 ± 0.3%, three replicates). Similarly, we observed good correspondence between the charging levels measured by Northern blot for $tRNA^{Ser}$(GCU) (68.1 ± 6.0, five biological replicates; 66.2 ± 1.0% by sequencing, three replicates) and $tRNA^{Thr}$(UGU) (74.6 ± 12.1%, five replicates; 75.7 ± 1.0% by sequencing, three replicates) (Figure 4C and D).

While our charged tRNA-seq method is not crucial for organisms with low tRNA sequence diversity (e.g. bacteria), determination of charging levels of tRNA isodecoders in mammals requires single-base resolution. The cause of or purpose for high tRNA diversity in mammals is not readily apparent. While tRNAs that are charged are most certainly used in translation, different isodecoders could potentially play distinct roles in translation. For example, different tRNA isodecoders of $tRNA^{Ser}$(UAG) show different stop codon suppression efficiency (20). Additionally, $tRNA^{Glu}$ isodecoders seem to have different mistranslation efficiency (21). A $tRNA^{Arg}$(UCU) isodecoder is specifically expressed in central nervous system, and its expression is needed to alleviate ribosome pausing (22). tRNA isodecoders can also have extra-translational functions. A $tRNA^{Asp}$ isodecoder that is not charged has been shown to bind to the 3′UTR of aspartyl-tRNA synthetase (AspRS) transcript in HeLa cells to regulate polyadenylation, mRNA stability, and AspRS translation (23). However, the individual functions of the vast majority of tRNA isodecoders have not yet been investigated. The intriguing result that some tRNA isodecoders have a much lower charging fraction (Figure 3B) could potentially signal that these tRNA have extra-translational functions, and these isodecoders may be candidates for future studies for tRNA 'moonlighting' functions.

In summary, we show that the charging fractions of tRNA isodecoders can be determined in a one-pot reaction using DM-tRNA-seq. Our high-throughput, high-resolution method to determine the charged fraction of tRNA isodecoders will allow for investigation into differences in charging levels under different cellular conditions such as stress or environmental perturbation.

DATA DEPOSITION

The sequencing data have been deposited in NCBI Geo database (accession GSE97259).

SUPPLEMENTARY DATA

Supplementary Data are available at NAR Online.

FUNDING

National Institutes of Health (NIH) [RM1HG008935 to T.P.]. NIH Chemistry and Biology Training Grant [T32

GM008720 to M.E.E., W.C.C.]; National Science Foundation Pre-doctoral Fellowship [DGE-1144082 to M.E.E.]. Funding for open access charge: NIH [RM1HG008935 to T.P.].
Conflict of interest statement. None declared.

REFERENCES

1. Dittmar,K.A., Sørensen,M.A., Elf,J., Ehrenberg,M. and Pan,T. (2005) Selective charging of tRNA isoacceptors induced by amino-acid starvation. *EMBO Rep.*, **6**, 151–157.
2. Elf,J., Nilsson,D., Tenson,T. and Ehrenberg,M. (2003) Selective charging of tRNA isoacceptors explains patterns of codon usage. *Science*, **300**, 1718–1722.
3. Subramaniam,A.R., Pan,T. and Cluzel,P. (2013) Environmental perturbations lift the degeneracy of the genetic code to regulate protein levels in bacteria. *Proc. Natl. Acad. Sci. U.S.A.*, **110**, 2419–2424.
4. Avcilar-Kucukgoze,I., Bartholomäus,A., Cordero Varela,J.A., Kaml,R.F.-X., Neubauer,P., Budisa,N. and Ignatova,Z. (2016) Discharging tRNAs: a tug of war between translation and detoxification in Escherichia coli. *Nucleic Acids Res.*, **44**, 8324–8334.
5. Haseltine,W.A. and Block,R. (1973) Synthesis of guanosine tetra- and pentaphosphate requires the presence of a codon-specific, uncharged transfer ribonucleic acid in the acceptor site of ribosomes. *Proc. Natl. Acad. Sci. U.S.A.*, **70**, 1564–1568.
6. Dever,T.E., Feng,L., Wek,R.C., Cigan,A.M., Donahue,T.F. and Hinnebusch,A.G. (1992) Phosphorylation of initiation factor 2α by protein kinase GCN2 mediates gene-specific translational control of GCN4 in yeast. *Cell*, **68**, 585–596.
7. Zhou,Y., Goodenbour,J.M., Godley,L.A., Wickrema,A. and Pan,T. (2009) High levels of tRNA abundance and alteration of tRNA charging by bortezomib in multiple myeloma. *Biochem. Biophys. Res. Commun.*, **385**, 160–164.
8. Varshney,U., Lee,C.P. and RajBhandary,U.L. (1991) Direct analysis of aminoacylation levels of tRNAs in vivo. Application to studying recognition of Escherichia coli initiator tRNA mutants by glutaminyl-tRNA synthetase. *J. Biol. Chem.*, **266**, 24712–24718.
9. McClain,W.H., Jou,Y.Y., Bhattacharya,S., Gabriel,K. and Schneider,J. (1999) The reliability of in vivo structure-function analysis of tRNA aminoacylation. *J. Mol. Biol.*, **290**, 391–409.
10. Sørensen,M.A. (2001) Charging levels of four tRNA species in Escherichia coli Rel+ and Rel− strains during amino acid starvation: a simple model for the effect of ppGpp on translational accuracy11Edited by D. E. Draper. *J. Mol. Biol.*, **307**, 785–798.
11. Zaborske,J.M., Narasimhan,J., Jiang,L., Wek,S.A., Dittmar,K.A., Freimoser,F., Pan,T. and Wek,R.C. (2009) Genome-wide analysis of tRNA charging and activation of the eIF2 kinase Gcn2p. *J. Biol. Chem.*, **284**, 25254–25267.
12. Goodenbour,J.M. and Pan,T. (2006) Diversity of tRNA genes in eukaryotes. *Nucleic Acids Res.*, **34**, 6137–6146.
13. Parisien,M., Wang,X. and Pan,T. (2014) Diversity of human tRNA genes from the 1000-genomes project. *RNA Biol.*, **10**, 1853–1867.
14. Zheng,G., Qin,Y., Clark,W.C., Dai,Q., Yi,C., He,C., Lambowitz,A.M. and Pan,T. (2015) Efficient and quantitative high-throughput tRNA sequencing. *Nat. Meth.*, **12**, 835–837.
15. Cozen,A.E., Quartley,E., Holmes,A.D., Hrabeta-Robinson,E., Phizicky,E.M. and Lowe,T.M. (2015) ARM-seq: AlkB-facilitated RNA methylation sequencing reveals a complex landscape of modified tRNA fragments. *Nat. Meth.*, **12**, 879–884.
16. Wolfson,A.D. and Uhlenbeck,O.C. (2002) Modulation of tRNAAla identity by inorganic pyrophosphatase. *Proc. Natl. Acad. Sci. U.S.A.*, **99**, 5965–5970.
17. Chan,P.P. and Lowe,T.M. (2009) GtRNAdb: a database of transfer RNA genes detected in genomic sequence. *Nucleic Acids Res.*, **37**, D93–D97.
18. Mohr,S., Ghanem,E., Smith,W., Sheeter,D., Qin,Y., King,O., Polioudakis,D., Iyer,V.R., Hunicke-Smith,S., Swamy,S. *et al.* (2013) Thermostable group II intron reverse transcriptase fusion proteins and their use in cDNA synthesis and next-generation RNA sequencing. *RNA*, **19**, 958–970.
19. Clark,W.C., Evans,M.E., Dominissini,D., Zheng,G. and Pan,T. (2016) tRNA base methylation identification and quantification via high-throughput sequencing. *RNA*, **22**, 1771–1784.
20. Geslain,R. and Pan,T. (2010) Functional Analysis of Human tRNA Isodecoders. *J. Mol. Biol.*, **396**, 821–831.
21. Gomes,A.C., Kordala,A.J., Strack,R., Wang,X., Geslain,R., Delaney,K., Clark,W.C., Keenan,R. and Pan,T. (2016) A dual fluorescent reporter for the investigation of methionine mistranslation in live cells. *RNA*, **22**, 467–476.
22. Ishimura,R., Nagy,G., Dotu,I., Zhou,H., Yang,X.-L., Schimmel,P., Senju,S., Nishimura,Y., Chuang,J.H. and Ackerman,S.L. (2014) Ribosome stalling induced by mutation of a CNS-specific tRNA causes neurodegeneration. *Science*, **345**, 455–459.
23. Rudinger-Thirion,J., Lescure,A., Paulus,C. and Frugier,M. (2011) Misfolded human tRNA isodecoder binds and neutralizes a 3′ UTR-embedded Alu element. *Proc. Natl. Acad. Sci. U.S.A.*, **108**, E794–E802.